Properties of CrN thin films deposited in plasma activated ABS by reactive magnetron sputtering

Paulo Pedrosa, Marco S. Rodrigues, Miguel A. Neto, Filipe J. Oliveira, Rui F. Silva, Joel Borges, Margarida Amaral, António Ferreira, Luís H. Godinho, Sandra Carvalho, Filipe Vaz

PII: S0257-8972(18)30650-9
DOI: doi:10.1016/j.surfcoat.2018.06.072
Reference: SCT 23526

To appear in: *Surface & Coatings Technology*

Received date: 23 March 2018
Revised date: 4 June 2018
Accepted date: 5 June 2018

Please cite this article as: Paulo Pedrosa, Marco S. Rodrigues, Miguel A. Neto, Filipe J. Oliveira, Rui F. Silva, Joel Borges, Margarida Amaral, António Ferreira, Luís H. Godinho, Sandra Carvalho, Filipe Vaz , Properties of CrN thin films deposited in plasma activated ABS by reactive magnetron sputtering. Sct (2018), doi:10.1016/j.surfcoat.2018.06.072

Properties of CrN thin films deposited in plasma activated ABS by reactive magnetron sputtering

Paulo Pedrosa[1,2,*], Marco S. Rodrigues[1], Miguel A. Neto[3], Filipe J. Oliveira[3], Rui F. Silva[3], Joel Borges[1], Margarida Amaral[4], António Ferreira[4], Luís H. Godinho[4], Sandra Carvalho[1], Filipe Vaz[1]

[1]*Centro de Física, Universidade do Minho, Campus de Gualtar, 4710-057 Braga, Portugal*

[2]*Institut FEMTO-ST, UMR 6174 CNRS, Université Bourgogne Franche-Comté, 15B Avenue des Montboucons, 25030 Besançon Cedex, France*

[3]*Department of Materials and Ceramic Engineering, CICECO, University of Aveiro, 3810-193 Aveiro, Portugal*

[4]*Prirev – Revestimentos Técnicos, Lda., Zona Industrial de Vagos – Lote 61, 3840-385 Vagos, Portugal*

[*] Corresponding author: Paulo Pedrosa; email address: paulo.pedrosa@fisica.uminho.pt; Centro de Física, Universidade do Minho, Campus de Gualtar, 4710-057 Braga, Portugal

Highlights

- CrN films were DC sputtered in Ar plasma activated ABS with increasing N_2 flows and deposition times

- Dense, smooth and amorphous films were obtained with 3 sccm N_2, 20 min deposition

- 3 sccm N_2, 20 min films display higher oxidation resistance and nobler OCP values

- The pre-sputtering Ar plasma treatment enhances adhesion of the 3 sccm N_2, 20 min film

- The 3 sccm N_2, 20 min film complies well with all end-user requirements

Abstract

In this work, magnetron sputtered CrN_x thin films with nitrogen concentrations ranging from 17 to 30 at. % were deposited on plasma activated ABS. Two sets of thin films were obtained by varying the N_2 flow inside the vacuum chamber (series #1) and the deposition time (series #2). The polymer samples were also subjected to plasma treatment in Ar prior to the CrN_x thin films' deposition, in order to enhance the adhesion. The fundamental microstructural, chemical and physical properties, as well as the electrochemical and adhesion behavior of the CrN_x thin films, were assessed by SEM, XRD, 3D profilometry, RAMAN, colorimetry, OCP measurements and cross-cut tape test. Main results show that high-quality CrN_x films with a low percentage of defects were obtained. The CrN_x film sputtered with 3 sccm N_2 for 20 min was considered to possess the most appropriate brightness, color, electrochemical stability and interfacial adhesion to fit the end-user requirements. Magnetron sputtering is thus a promising alternative to the hazardous chrome plating for an effective metallization of ABS.

Keywords: Sputtering; Chromium nitride; ABS; Metallization; Polymer coating.

1. Introduction

Thin film-coated (metallized) polymers are replacing traditional metallic materials in many industrial fields, particularly in automotive [1], electronic [2], and wear protection applications [3]. The low density, flexibility, design versatility and low-cost production of most polymers [1,4], combined with the properties of a shining, highly reflective and conductive metallic coating, gives them a considerable advantage over common metals [5].

Acrylonitrile Butadiene Styrene (ABS) is widely used in industrial applications such as automotive, electronic housings, computer and air conditioning parts [3]. This is due to its intrinsic properties, in particular an outstanding impact resistance, good processability and dimensional stability, recyclability, and cost-effectiveness [1,3,5,6]. As such, ABS dominates the market of metallized polymers [1].

One of the most common polymer metallization processes used in the last decades has been electroplating that produces environmentally dangerous waste products, such as the highly toxic hexavalent chromium used either in the surface activation/etching step [7] or in the chrome plating itself [5]. Hence, following all the enacted European legislation during the last years against the use of hexavalent chromium solutions [8,9], new chromium surface treatments [1] and plating alternatives have emerged and include chemical, physical, and mixed approaches [1,3,5].

Magnetron sputtering (MS) is one of such techniques [3,10,11], which can be used on a wide range of available polymers and has a reduced environmental impact, unlike chrome plating [12]. MS advantages and disadvantages over electroplating are effectively summarized in reference [13]. Electroless plating has the advantage of being capable of levelling the coated surface, which may lead to a superior decorative finishing and brightness, while the most attractive feature of MS may be the ability to coat most substrate materials with a wide range of thin film systems in an environmentally friendly and cost-effective way. Consequently, MS

is becoming an increasingly attractive industrial process for polymer metallization, especially for the deposition of chromium nitride (CrN) films [14–18] for protective and decorative purposes [3,11,19]. Furthermore, MS allows for a simple and fine control of the process parameters (pressure, temperature, current, etc.) thus allowing an effective tailoring of the CrN thin film microstructures and properties obtained [19,20], especially in polymers that are rather susceptible to high temperatures developed during the sputtering process [21]. Consequently, MS chrome metallization of ABS is an excellent alternative to electroplating since it allows the deposition of thin films with superior corrosion resistance, and mechanical and tribological properties [22–27].

In the present work, the authors aim at developing an environmentally friendly MS-based process for ABS chrome metallization that is able to deposit CrN films with protective and decorative properties comparable to the ones obtained traditionally by electroplating. As such, several end-user requirements such as the deposition of well-adhered, dense, defect-free, bright and reflective films with high chemical and electrochemical stability must be attained.

2. Experimental details

CrN thin films were fabricated by DC magnetron sputtering using a pure chromium target (200×100×6 mm^3, 99.99% purity), in a custom-made 60 L vacuum chamber. All depositions were performed after a residual vacuum of approximately 10^{-4} Pa is attained inside the reactor. During the sputtering process, the gas atmosphere was composed of a mixture of Ar (φ = 25 sccm, p = 3.8×10^{-1} Pa) and N_2 ($0 \leq \varphi \leq 8$ sccm, partial pressure varied 0.5 Pa). The plasma was ignited using a current density of 75 $A\cdot m^2$. The grounded sample holder was used in rotation mode at 5 rpm in front of the target ($d_{target\text{-}sample}$ = 7 cm). No external heating was used. The coated substrates were silicon (Boron-doped, p-type, <100> orientation, 525 μm thick) for chemical, morphological and (micro)structural characterization purposes, glass for

the electrochemical behavior, ABS for color, brightness and reflectance measurements, and PET and PA for adhesion. Before all depositions, the surface of the substrates was subjected to a plasma treatment using a 40 kHz RF generator with a power of 100 W in an argon atmosphere (80 Pa for 5 min) for surface activation in a Low-Pressure Plasma Cleaner by Diener Electronic (Zepto Model). No sample bias was used in the pre-cleaning step. Further details regarding the plasma treatment and deposition process of both series of films are patent in Table I.

The surfaces of the sputtered samples had to comply with several end-user requirements, hence the performed characterization was specifically selected to target the desired thin film specifications. The morphological features were observed under a Hitachi SU70 Scanning Electron Microscope (SEM), equipped with a Bruker Energy Dispersion Spectroscopy (EDS) system used to assess the nitrogen incorporation in the films, and operated at 15 kV. The X-ray diffraction (XRD) technique was used to access the crystalline nature of the coatings. This analysis was performed on a XPERT-PRO diffractometer in blazing angle mode with 2θ between 20º and 80º. Topographic analysis was done using a 3D optical profilometer (Sensofar S-neox) to assess the surface roughness of the plasma treated coated materials. Data were obtained with a 10x interferometric objective (acquisition area of 1.75 mm × 1.35 mm) using the vertical shift interferometry technique (VSI). The visualization of the surface texture was also done using a higher magnification (100x objective – acquisition area of 350 μm × 270 μm) under confocal mode. Finally, Raman spectra were obtained for these CrN coatings on a confocal Raman-AFM-SNOM WITec alpha300 RAS+ microscope. The excitation source was the 532 nm line of a Nd:YAG laser with 5 mW incident power on the samples. The spectra were obtained in the Stokes shifts interval between 80-2000 cm^{-1}.

Open circuit potential (OCP) measurements were performed in a 0.9% NaCl solution for 3h to mimic the performance of the more promising coatings deposited in glass slides and PET in

high humidity and saline environments, using a saturated calomel electrode (SCE) in a Gamry Reference 600 potentiostat (Gamry Instruments Inc., PA, USA). The color coordinates of the films were measured in the silicon <100> substrates, using a Minolta CM-2600d portable spectrophotometer equipped with a 52 mm diameter integrating sphere and 3 pulsed xenon lamps and a wavelength range of 400 – 700 nm. The color coordinates were measured in ABS pieces provided by the end-user and were represented in the CIELab-1976 color space at a viewing angle of 10º and using the primary illuminant D65 (specular component included – SCI). Flat PET substrates were used for the cross-cut tape test on the film that best complied with the end-user specifications, based on the ASTM D3359-B standard.

3. Results and discussion

3.1. Morphological, Microstructural and Chemical characterization

The morphological features of the sputtered CrN samples from series #1 and #2 are present in Fig. 1 and 2, respectively. For the pure Cr reference sample it is possible to observe the occurrence of a typical elongated granular morphology, Fig. 1a [28]. The resulting morphology is quite rough (Sa = 42 nm, Fig. 3 a) and consists of a highly oriented and crystalline Cr (210) growth (card #65-3316), Fig. 4 a.

By introducing small amounts of nitrogen (2 and 3 sccm) in the system, round granular morphologies are obtained [28–30], Fig. 1 b-c. Since the obtained surfaces are dense and very smooth [30] (Sa ≈ 21 nm for both samples, Fig. 3 a) the magnification of Fig. 1 c is higher in order to observe the round granules. Due to the low nitrogen amount (nitrogen composition ≈ 17 at. %), a low-crystallinity microstructure – slight nitrogen incorporation in the chromium matrix (the broad peak at ≈ 42º corresponds to the Cr_2N (002) phase, card #35-803) – is obtained for the 2 sccm N_2 sample, while an almost amorphous growth is visible for the 3

sccm N_2 film, Fig. 4 a. With further nitrogen increase (4 sccm), the surface morphology of the samples starts to change, and the smooth, granular features become increasingly sharp and angular, Fig. 1 d. As a result, the roughness slightly increases (Sa ≈ 26 nm, Fig. 3) due to an increasingly N-rich crystalline Cr_2N (002) preferential growth, Fig. 4 a.

For high nitrogen flow rates, higher nitrogen incorporation occurs (≈ 29 and 25 at. % for 6 and 8 sccm, respectively – Table I). Consequently, evidences of pyramid-like column tops (typical for high N_2 contents [31]) start to appear in the sample sputtered with 6 sccm and are fully formed in the CrN film deposited with 8 sccm, Fig. 1 e, f. Therefore, the surface roughness remains higher (24 ≤ Sa ≤ 25 nm) than that of the intermediate-N_2 films (2 and 3 sccm; Sa ≈ 21 nm) but slightly lower that the values obtained for the 4 sccm sample (Sa ≈ 26 nm), Fig. 3. The high-N_2 samples are also more porous than the low- and intermediate-N_2 films. The progressive evolution from an N-deficient Cr_2N (002) with traces of amorphous Cr (210) phase of the sample sputtered with 6 sccm, towards a fully crystalline CrN (111), (200), (220) and (311) microstructure (card #65-2899) with no evidences of metallic Cr of the 8 sccm coating is evident [3], Fig. 4 a. A change from the CrN (111) preferential growth to the (220) phase also occurs.

Consequently, the films deposited with 2 and 3 sccm N_2 were considered the most promising and thus, due to their similar morphological and microstructural behavior, a nitrogen flow rate of 3 sccm was fixed and the deposition time was varied from 10 to 60 min in order to sputter the series #2 films, Fig. 2. Rougher (30 ≤ Sa ≤ 35 nm) and slightly more porous films are obtained for high depositions times (30-60 min), in opposition to the denser and smoother (21 ≤ Sa ≤ 26 nm) CrN coatings sputtered for 10 and 20 min, Fig. 3. All series #2 films display a granular-like morphology due to low nitrogen incorporation. However, an increase of the nitrogen uptake from ≈ 13 to ≈ 23 at. % occurs with increasing deposition times, Table I. Consequently, a gradual evolution from an amorphous microstructure – 10 and 20 min –

towards N-deficient Cr_2N (002) – 30 min – and finally to a poorly crystallized CrN (200) growth – 40 and 60 min – is observed, Fig 4 b.

The RAMAN analysis of all sputtered samples is shown in Fig. 5. In the pure Cr and low-N_2 films (2 and 3 sccm), no defined Raman peaks can be detected, Fig. 5 a. Instead, a broad band around 620 cm^{-1} is seen that can be indexed to the formation of Cr_2O_3 [32], which is indicative of slight oxidation of these samples when exposed to ambient air. Also traces of hexagonal Cr_2N phase can be indexed to the band located at 215 cm^{-1} in the film sputtered with 3 sccm N_2, which is consistent with the XRD results, Fig. 4 a. With increasing nitrogen flow rate/concentration – 4, 6 and 8 sccm – further extensive oxidation is detected due to the presence of sharp Cr_2O_3 peaks at 304, 342 and 540 cm^{-1} [33–35]. Once more, the results are consistent with the morphological and microstructural findings, since the surface porosity increases with the increase of nitrogen incorporation (Fig. 1 d-f) due to the gradual shift from a dense N-deficient amorphous Cr_2N structure towards porous crystalline CrN, Fig. 4. No significant oxidation was detected with increasing deposition times, Fig. 5 b.

3.2. Optical, Electrochemical and Adhesion characterization

The color coordinates and reflectance of the films from series #1 and #2 were studied in order to check if the deposited coatings complied with end-user specifications. The color coordinates are shown in Fig. 6. With the increase of the nitrogen flow rate (and incorporation), the brightness (L* coordinate) of the samples suffer an overall decrease, while the films obtained with 2 and 3 sccm N_2 exhibit the highest L* values. This occurs since the films suffer a color change from metallic (0, 2 and 3 sccm N_2) towards yellow/brown typical for intermediate- and high-N_2 content CrN (4, 6 and 8 sccm N_2), confirmed by the steep increase of b* (b* > 0 refers to yellow) and slight increase of a* (a* > 0 refers to red). Also,

the porosity and roughness increase also plays an important part due to scattering of the visible light [36]. Consequently, the low-N_2 films (2 and 3 sccm) display higher reflectance values in the visible range than the intermediate- (4 sccm) and high-N_2 (6 and 8 sccm) samples, Fig. 7 a.

Since an uptake of nitrogen was detected with increasing deposition times, only slight variations of L* and b* are visible, Fig. 6 b. However, these variations are within the 5% measurement error, expect for the brightness of the films obtained with 40 and 60 min, due to their increased roughness, Fig. 3 a. The reflectance behavior is consistent with the previous results, with the samples sputtered with high deposition times exhibiting significantly lower reflectance values than the ones deposited for 10-30 min, Fig. 7 b.

Once more, similarly to the results obtained in sections 3.1., the CrN films deposited with low nitrogen flow rates – 2 and 3 sccm (≈ 17 at. % N_2) – and low deposition times – 10 to 30 min – comply with end-user specifications (smooth, dense, bright and reflective CrN coatings). Consequently, these samples (2 and 3 sccm N_2, 20 min deposition) were immersed in a 0.9% NaCl solution to study the evolution of the electrochemical OCP values, Fig. 8, thus mimicking the surface stability in moist and saline conditions (i.e. human manipulation and handling). Both potentials are quite stable varying from 59-72 mV and 147-155 mV for the 2 and 3 sccm N_2 films, respectively. Moreover, it is possible to see that the OCP values of the CrN film sputtered with 3 sccm N_2 are much nobler that the ones exhibited by the 2 sccm N_2 coating and thus less prone to surface oxidation and corrosion [37–39]. Therefore, combining all results so far, the sample sputtered with 3 sccm N_2 film for 20 min was selected to be sputtered in flat PET substrates. The electrochemical stability of the OCP values of this sample was also analyzed, Fig. 8. As expected, the exhibited values are slightly less noble and less stable (varying from 38 to 72 mV) due to the poor surface finishing of the PET flat

samples (not polished) when compared to the smooth glass slides. Nevertheless, the displayed OCP values are more than acceptable for the envisaged use.

One of the most important end-user specifications was that the deposited CrN films were well adhered to the polymeric substrate. Therefore, the adhesion of the most promising CrN film (3 sccm N_2 and 20 min deposition) was studied using the cross-cut tape test, according to the ASTM D3359-B standard (which provides a decreasing adhesion classification between a maximum 5B and minimum 0B) and the results are patent in Fig. 9. Since no flat ABS pieces were available for this study (flatness of the samples is important for a correct use of the ASTM norm), the tests were conducted in flat PET substrates. It is possible to see that the pre-deposition plasma treatment (Table I) is able to promote excellent adhesion levels of the 3 sccm N_2, 20 min deposition film in PET (Fig. 9 a, b). This is due to extensive topographic (roughness promotion) and chemical (chain scission, formation of oxygen dangling bonds and oxygen-containing reactive groups) changes promoted by the Ar bombardment in the outer layers of the polymer substrates, as evidenced in previous works by the authors [40–43]. Hence, according to the scale defined by the used norm, the adhesion of the CrN film deposited with 3 sccm N_2 for 20 min can be rated as 5B (maximum), since the edges of the cuts are completely smooth and none of the squares of the lattice is detached after removal of the tape [43], Fig. 9 b. The film was also sputtered in ABS pieces bur since they have a complex shape and are not flat, the cross-cut tape test could not be performed effectively. However, the coated ABS pieces exhibit a good superficial aspect and do not present cracks or delamination.

4. Conclusion

Two series of CrN films were sputtered with increasing nitrogen flow rates (2-8 sccm)/contents (17-29 at. %) and deposition times (10-60 min). The morphological, microstructural and chemical properties were investigated and then correlated with the exhibited color, electrochemical stability and adhesion behavior. Main results show that the intermediate- and high N_2 porous films (4, 6 and 8 sccm) are easily oxidized in ambient air and do not comply with other end-user requirements such as brightnes and reflectance, thus not being suitable for decorative use. In opposition, the dense low-N_2 coatings (2 and 3 sccm) do not suffer extensive surface oxidation due to air exposure and also exhibit bright and reflective surfaces. However, the 2 sccm N_2 film displays less noble OCP values that the 3 sccm N_2 sample, thus being more susceptible to oxidation when exposed to moist and saline conditions (i.e. human manipulation and handling). Consequently, the film sputtered with 3 sccm N_2 for 20 min was considered the most promising to coat ABS pieces since they comply with all end-user requirements: dense, defect-free, bright and reflective surfaces that are chemically and electrochemically stable, while being well-adhered to the base substrate.

Acknowledgements

This work was developed within the scope of the project POCI-01-0247-FEDER-003493 co-financed by FEDER through the POCI program and project CICECO-Aveiro Institute of Materials, POCI-01-0145-FEDER-007679 (FCT ref. UID/CTM/50011/2013), financed by national funds through FCT/MEC and when appropriate co-financed by FEDER under the PT2020 Partnership Agreement.

References

[1] D. Chen, Z. Kang, ABS plastic metallization through UV covalent grafting and layer-by-layer deposition, Surf. Coatings Technol. 328 (2017) 63–69. doi:10.1016/j.surfcoat.2017.08.020.

[2] Z. Wang, Q. Li, W. Trinh, Q. Lu, H. Cho, Q. Wang, L. Chen, Optimal design of high temperature metalized thin-film polymer capacitors: A combined numerical and experimental method, J. Power Sources. 357 (2017) 149–157. doi:10.1016/J.JPOWSOUR.2017.04.087.

[3] P. Sukwisute, R. Sakdanuphab, A. Sakulkalavek, Hardness and wear resistance improvement of ABS surface by CrN thin film, Mater. Today Proc. 4 (2017) 6553–6561. doi:10.1016/j.matpr.2017.06.167.

[4] A. Patil, A. Patel, R. Purohit, An overview of Polymeric Materials for Automotive Applications, Mater. Today Proc. 4 (2017) 3807–3815. doi:10.1016/J.MATPR.2017.02.278.

[5] A. Garcia, T. Berthelot, P. Viel, A. Mesnage, P. Jégou, F. Nekelson, S. Roussel, S. Palacin, ABS Polymer Electroless Plating through a One-Step Poly(acrylic acid) Covalent Grafting, ACS Appl. Mater. Interfaces. 2 (2010) 1177–1183. doi:10.1021/am1000163.

[6] M. Rahimi, M. Esfahanian, M. Moradi, Effect of reprocessing on shrinkage and mechanical properties of ABS and investigating the proper blend of virgin and recycled ABS in injection molding, J. Mater. Process. Technol. 214 (2014) 2359–2365. doi:10.1016/J.JMATPROTEC.2014.04.028.

[7] X. Tang, J. Wang, C. Wang, B. Shen, A novel surface activation method for Ni/Au electroless plating of acrylonitrile–butadiene–styrene, Surf. Coatings Technol. 206 (2011) 1382–1388. doi:10.1016/J.SURFCOAT.2011.08.064.

[8] Directive 2002/95/EC of the European Parliament and of the Council, Off. J. Eur. Union. L 37 (2003) 19-23. http://data.europa.eu/eli/dir/2002/95/oj

[9] Directive 2005/90/EC of the European Parliament and of the Council, Off. J. Eur. Union. L 33 (2006) 28–81. http://data.europa.eu/eli/dir/2005/90/oj

[10] A. Höflich, N. Bradley, C. Hall, D. Evans, P. Murphy, E. Charrault, Packing density/surface morphology relationship in thin sputtered chromium films, Surf. Coatings Technol. 291 (2016) 286–291. doi:10.1016/J.SURFCOAT.2016.02.061.

[11] J.M. Lackner, W. Waldhauser, C. Ganser, C. Teichert, M. Kot, L. Major, Mechanisms of topography formation of magnetron-sputtered chromium-based coatings on epoxy polymer composites, Surf. Coatings Technol. 241 (2014) 80–85. doi:10.1016/J.SURFCOAT.2013.07.040.

[12] B. Navinšek, P. Panjan, I. Milošev, PVD coatings as an environmentally clean alternative to electroplating and electroless processes, Surf. Coatings Technol. 116–119 (1999) 476–487. doi:10.1016/S0257-8972(99)00145-0.

[13] H.A. Jehn, PVD and ECD-competition, alternative or combination?, Surf. Coatings Technol. 112 (1999) 210–216. doi:10.1016/S0257-8972(98)00750-6.

[14] A. Garzon-Fontecha, H.A. Castillo, E. Restrepo-Parra, W. De La Cruz, The role of the nitrogen flow rate on the transport properties of CrN thin films produced by DC magnetron sputtering, Surf. Coatings Technol. 334 (2018) 98–104. doi:10.1016/J.SURFCOAT.2017.11.009.

[15] F. Ferreira, J.C. Oliveira, A. Cavaleiro, CrN thin films deposited by HiPIMS in DOMS mode, Surf. Coatings Technol. 291 (2016) 365–375. doi:10.1016/J.SURFCOAT.2016.02.064.

[16] A. Lippitz, T. Hübert, XPS investigations of chromium nitride thin films, Surf. Coatings Technol. 200 (2005) 250–253. doi:10.1016/J.SURFCOAT.2005.02.091.

[17] P. Hones, N. Martin, M. Regula, F. L vy, Structural and mechanical properties of chromium nitride, molybdenum nitride, and tungsten nitride thin films, J. Phys. D. Appl. Phys. 36 (2003) 1023–1029. doi:10.1088/0022-3727/36/8/313.

[18] K. Ibrahim, M.M. Rahman, X. Zhao, J.-P. Veder, Z. Zhou, E. Mohammadpour, R.H. Majeed, A.N. Nikoloski, Z.-T. Jiang, Annealing effects on microstructural, optical, and mechanical properties of sputtered CrN thin film coatings: Experimental studies and finite element modeling, J. Alloys Compd. 750 (2018) 451–464. doi:10.1016/J.JALLCOM.2018.04.012.

[19] Y.-H. Yang, I.-W. Yeo, S.-J. Park, Y.-S. Oh, Microstructure and phase forming behaviour of chrome based multi-composition nitride coatings with nanolayer structures, Ceram. Int. 40 (2014) 11567–11573. doi:10.1016/j.ceramint.2014.03.114.

[20] Z.G. Zhang, O. Rapaud, N. Bonasso, D. Mercs, C. Dong, C. Coddet, Control of microstructures and properties of dc magnetron sputtering deposited chromium nitride films,

Vacuum. 82 (2008) 501–509. doi:10.1016/J.VACUUM.2007.08.009.

[21] K. Zuber, C. Hall, P. Murphy, D. Evans, Atomic structure studies of chrome alloy coatings and their abrasion resistance, Surf. Coatings Technol. 206 (2012) 3645–3649. doi:10.1016/j.surfcoat.2012.03.014.

[22] G. Li, P. Deshpande, J.H. Li, R.Y. Lin, Nano Cr interlayered CrN coatings on steels, Tsinghua Sci. Technol. 10 (2005) 690–698. doi:10.1016/S1007-0214(05)70137-1.

[23] R. Bayón, A. Igartua, X. Fernández, R. Martínez, R.J. Rodríguez, J.A. García, A. de Frutos, M.A. Arenas, J. de Damborenea, Corrosion-wear behaviour of PVD Cr/CrN multilayer coatings for gear applications, Tribol. Int. 42 (2009) 591–599. doi:10.1016/J.TRIBOINT.2008.06.015.

[24] J.A. Alegría-Ortega, L.M. Ocampo-Carmona, F.A. Suárez-Bustamante, J.J. Olaya-Flórez, Erosion–corrosion wear of Cr/CrN multi-layer coating deposited on AISI-304 stainless steel using the unbalanced magnetron (UBM) sputtering system, Wear. 290–291 (2012) 149–153. doi:10.1016/J.WEAR.2012.04.007.

[25] A. Ruden, E. Restrepo-Parra, A.U. Paladines, F. Sequeda, Corrosion resistance of CrN thin films produced by dc magnetron sputtering, Appl. Surf. Sci. 270 (2013) 150–156. doi:10.1016/J.APSUSC.2012.12.148.

[26] E. Bozyazı, M. Ürgen, A.F. Çakır, Comparison of reciprocating wear behaviour of electrolytic hard chrome and arc-PVD CrN coatings, Wear. 256 (2004) 832–839. doi:10.1016/S0043-1648(03)00523-4.

[27] A. Hurkmans, D.B. Lewis, W.D. Münz, Runner-Up Magnetron Sputtered CrN x Coatings as Alternative to Electroplated Hard Chromium, Surf. Eng. 19 (2003) 205–210. doi:10.1179/026708403225006140.

[28] Z. Qi, Z. Wu, D. Zhang, B. Wei, J. Wang, Z. Wang, Effect of sputtering power on the chemical composition, microstructure and mechanical properties of CrNx hard coatings deposited by reactive magnetron sputtering, Vacuum. 145 (2017) 136–143. doi:10.1016/J.VACUUM.2017.08.036.

[29] T. Elangovan, P. Kuppusami, R. Thirumurugesan, V. Ganesan, E. Mohandas, D. Mangalaraj, Nanostructured CrN thin films prepared by reactive pulsed DC magnetron sputtering, Mater. Sci. Eng. B. 167 (2010) 17–25. doi:10.1016/j.mseb.2010.01.021.

[30] G. Greczynski, J. Lu, O. Tengstrand, I. Petrov, J.E. Greene, L. Hultman, Nitrogen-doped bcc-Cr films: Combining ceramic hardness with metallic toughness and conductivity, Scr. Mater. 122 (2016) 40–44. doi:10.1016/J.SCRIPTAMAT.2016.05.011.

[31] Y.B. Gerbig, V. Spassov, A. Savan, D.G. Chetwynd, Topographical evolution of sputtered chromium nitride thin films, Thin Solid Films. 515 (2007) 2903–2920. doi:10.1016/j.tsf.2006.08.031.

[32] J.. Maslar, W.. Hurst, W.. Bowers, J.. Hendricks, M.. Aquino, I. Levin, In situ Raman spectroscopic investigation of chromium surfaces under hydrothermal conditions, Appl. Surf. Sci. 180 (2001) 102–118. doi:10.1016/S0169-4332(01)00338-5.

[33] A. Barata, L. Cunha, C. Moura, Characterisation of chromium nitride films produced by PVD techniques, Thin Solid Films. 398–399 (2001) 501–506. doi:10.1016/S0040-6090(01)01498-5.

[34] M. Arif, A. Sanger, A. Singh, Sputter deposited chromium nitride thin electrodes for supercapacitor applications, Mater. Lett. (2018), in press. doi:10.1016/j.matlet.2018.02.094.

[35] R. Kaindl, R. Franz, J. Soldan, A. Reiter, P. Polcik, C. Mitterer, B. Sartory, R. Tessadri, M. O'Sullivan, Structural investigations of aluminum-chromium-nitride hard coatings by Raman micro-spectroscopy, Thin Solid Films. 515 (2006) 2197–2202. doi:10.1016/j.tsf.2006.07.144.

[36] H.E. Bennett, J.O. Porteus, Relation Between Surface Roughness and Specular Reflectance at Normal Incidence, J. Opt. Soc. Am. 51 (1961) 123-129. doi:10.1364/JOSA.51.000123.

[37] G. Bertrand, H. Mahdjoub, C. Meunier, A study of the corrosion behaviour and protective quality of sputtered chromium nitride coatings, Surf. Coatings Technol. 126 (2000) 199–209. doi:10.1016/S0257-8972(00)00527-2.

[38] S. Han, J.H. Lin, S.H. Tsai, S.C. Chung, D.Y. Wang, F.H. Lu, H.C. Shih, Corrosion and tribological studies of chromium nitride coated on steel with an interlayer of electroplated chromium, Surf. Coatings Technol. 133–134 (2000) 460–465. doi:10.1016/S0257-8972(00)00979-8.

[39] T.J. Pan, B. Zhang, J. Li, Y.X. He, F. Lin, An investigation on corrosion protection of chromium nitride coated Fe–Cr alloy as a bipolar plate material for proton exchange

membrane fuel cells, J. Power Sources. 269 (2014) 81–87. doi:10.1016/j.jpowsour.2014.06.147.

[40] A. Ferreira, P. Pedrosa, S. Lanceros-Mendez, A. V Machado, F. Vaz, Activation of polyethylene terephthalate using different plasma treatments, J. Optoelectron. Adv. Mater. 12 (2010) 1581–1589.

[41] P. Pedrosa, J.-M. Chappé, C. Fonseca, A.V. Machado, J.M. Nóbrega, F. Vaz, Plasma Surface Modification of Polycarbonate and Poly(propylene) Substrates for Biomedical Electrodes, Plasma Process. Polym. 7 (2010) 676–686. doi:10.1002/ppap.200900176.

[42] P. Lima, P. Pedrosa, A.V. Machado, C. Fonseca, F. Vaz, Plasma Surface Activation and TiN Coating of a TPV Substrate for Biomedical Applications, Plasma Process. Polym. 8 (2011) 1174–1183. doi:10.1002/ppap.201100073.

[43] P. Pedrosa, P. Fiedler, C. Lopes, E. Alves, N.P. Barradas, J. Haueisen, A. V. Machado, C. Fonseca, F. Vaz, Ag:TiN-Coated Polyurethane for Dry Biopotential Electrodes: From Polymer Plasma Interface Activation to the First EEG Measurements, Plasma Process. Polym. 13 (2016) 341–354. doi:10.1002/ppap.201500063.

Table captions

Table I. Plasma treatment and MS deposition process parameters.

Plasma treatment (before all depositions)				
Ar (Pa)		**Power (W)**		**Time (s)**
80		100		300
Series #1 (1.5 A, 25 sccm Ar, 20 min.)				
Sample #	**U (V)**	**N_2 (sccm)**	**N composition (at. %)**	**Thickness (nm)**
1	284±1	0	-	340±50
2	308±1	2	17.4±5	370±50
3	309±1	3	16.8±5	146±50
4	305±1	4	23.1±5	230±50
6	304±1	6	29.2±5	490±50
8	303±1	8	25.1±5	230±50
Series #2 (1.5 A, 25 sccm Ar, 3 sccm N_2)				
Sample #	**U (V)**	**t_{dep} (min.)**	**N composition (at. %)**	**Thickness (nm)**
3	309±1	20	16.8±5	146±50
9	307±1	10	12.7±5	119±50
10	305±1	30	23.1±5	394±50
11	304±1	40	23.0±5	661±50
12	305±1	60	23.1±5	739±50

Figure captions

Figure 1. SEM top view micrographs of CrN films sputtered with increasing N_2 flow rates.

Figure 2. SEM top view micrographs of the CrN films deposited with increasing deposition times.

Figure 3. Roughness evolution (a) of series #1 and #2 CrN films. 2D (b,d) and 3D profilometry (c,e) images of the samples deposited with 2 sccm N_2 and 3 sccm N_2.

Figure 4. Structural evolution of the CrN films from series #1 and #2.

Figure 5. Raman spectra of the CrN films from series #1 and #2.

Figure 6. CIE L a* b* color coordinates of the sputtered CrN films.

Figure 7. Reflectance evolution of the CrN films from series #1 and #2.

Figure 8. OCP values of selected 2 and 3 sccm N_2 coatings.

Figure 9. Adhesion behavior assessment of the most promising CrN film: 3 sccm N_2, 20 min deposition.

Figure 1

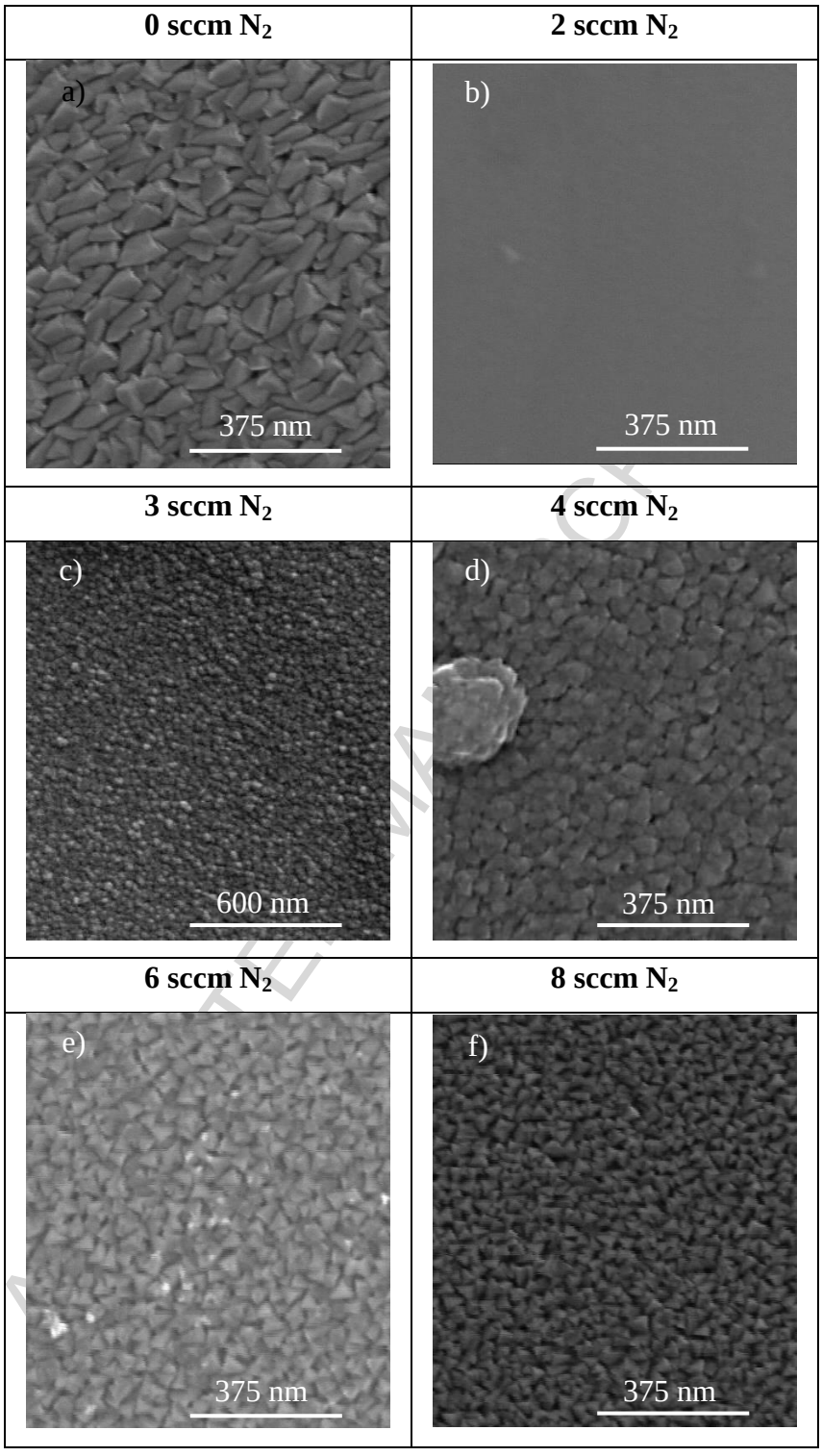

Figure 2

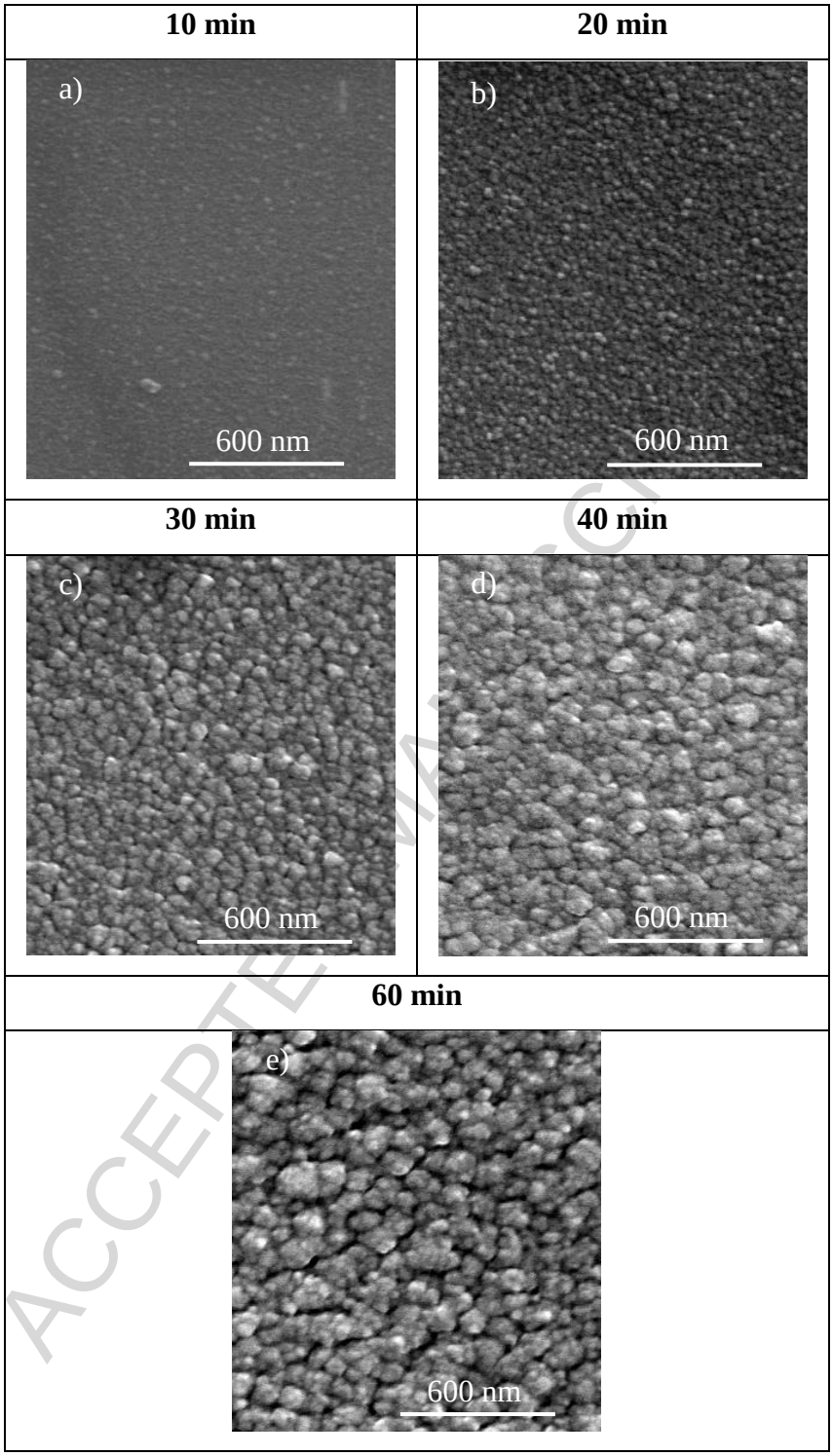

Figure 3

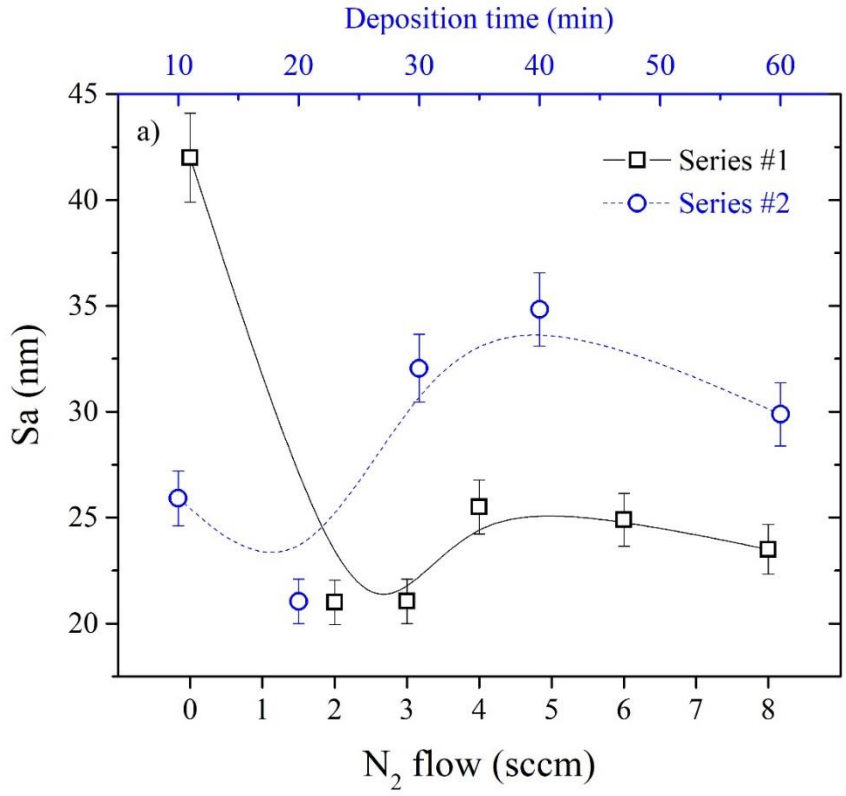

2 sccm N_2	3 sccm N_2
b) 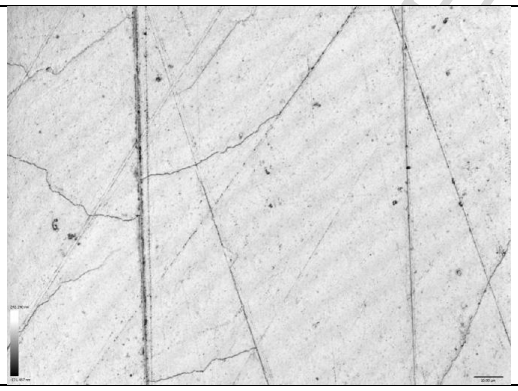	c) 
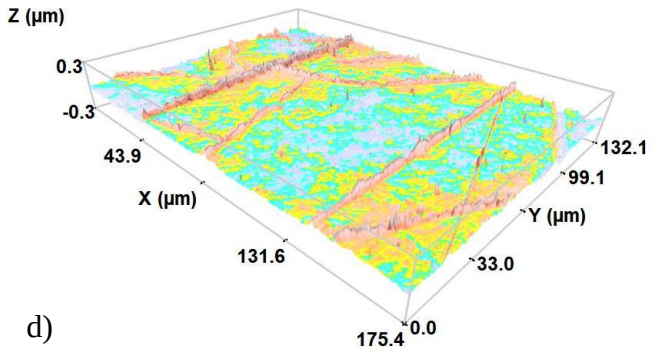 d)	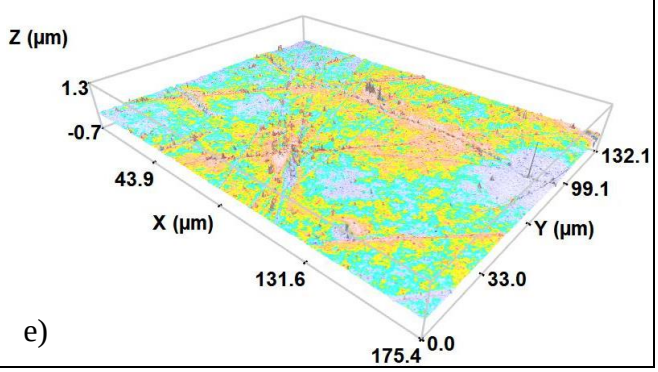 e)

Figure 4

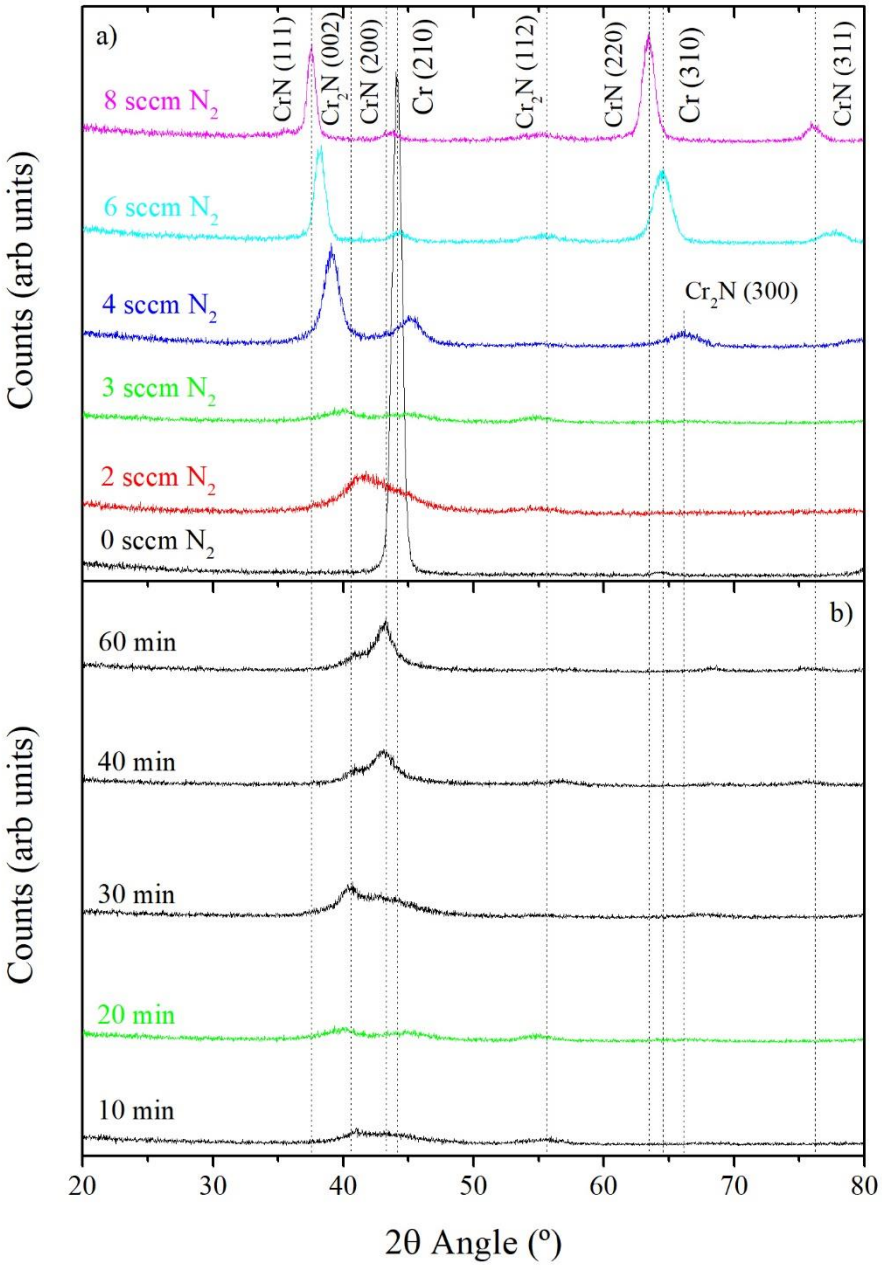

Figure 5

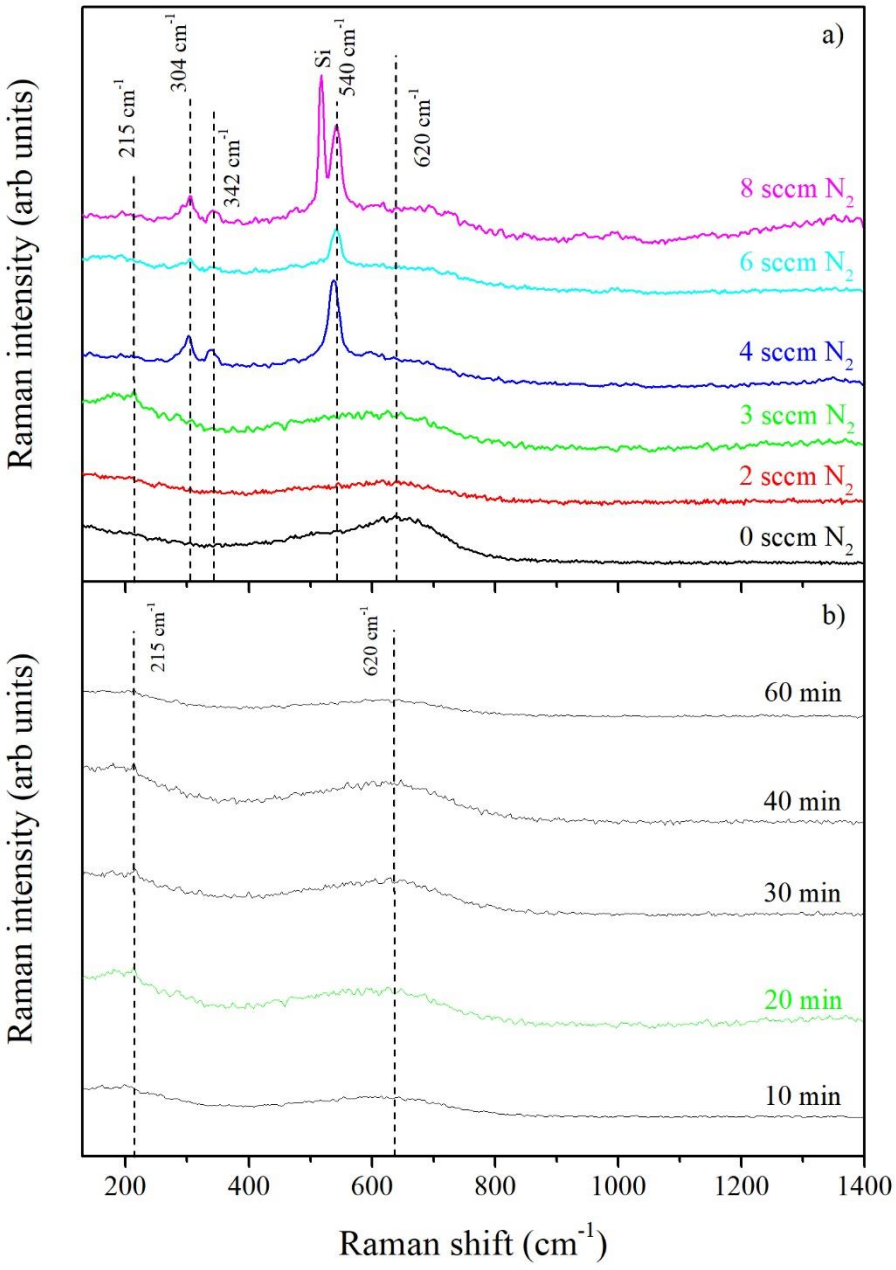

Figure 6

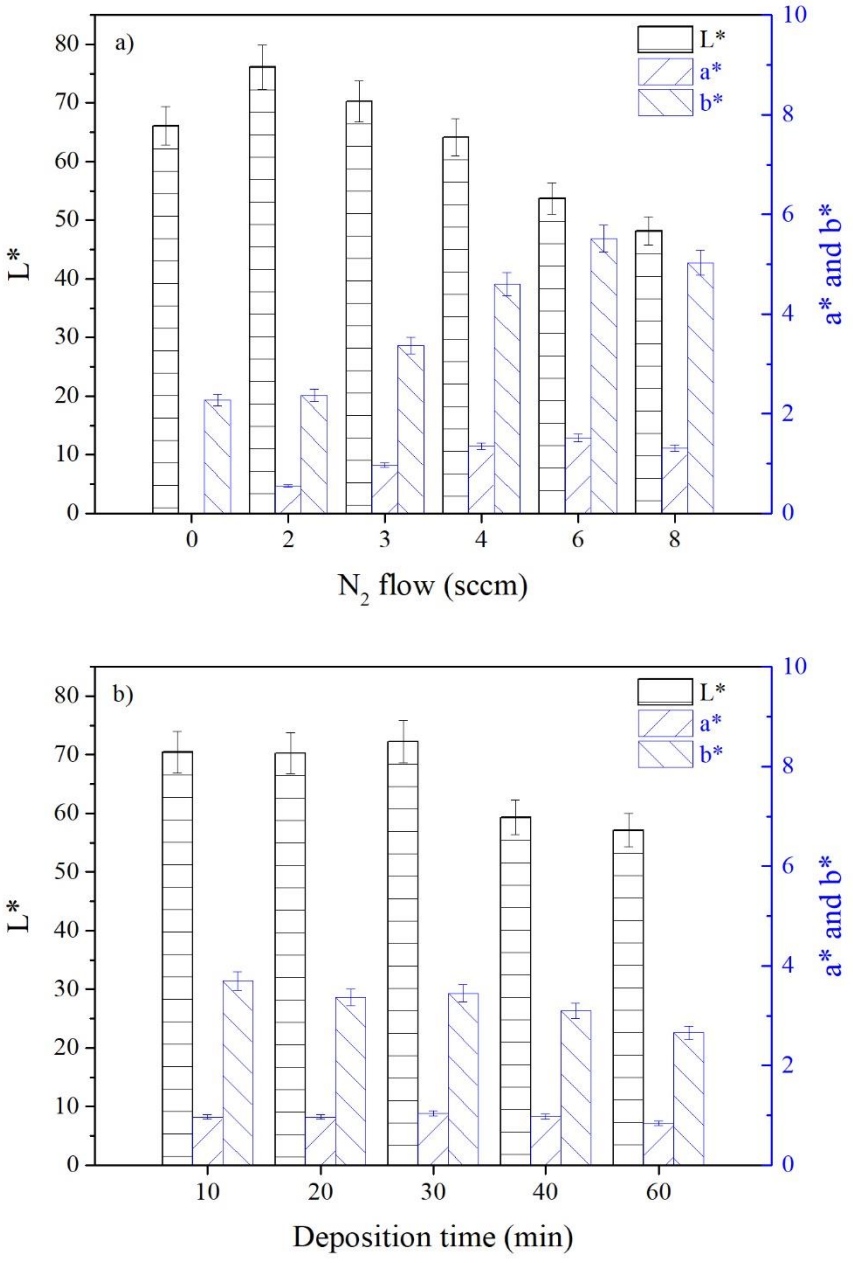

Figure 7

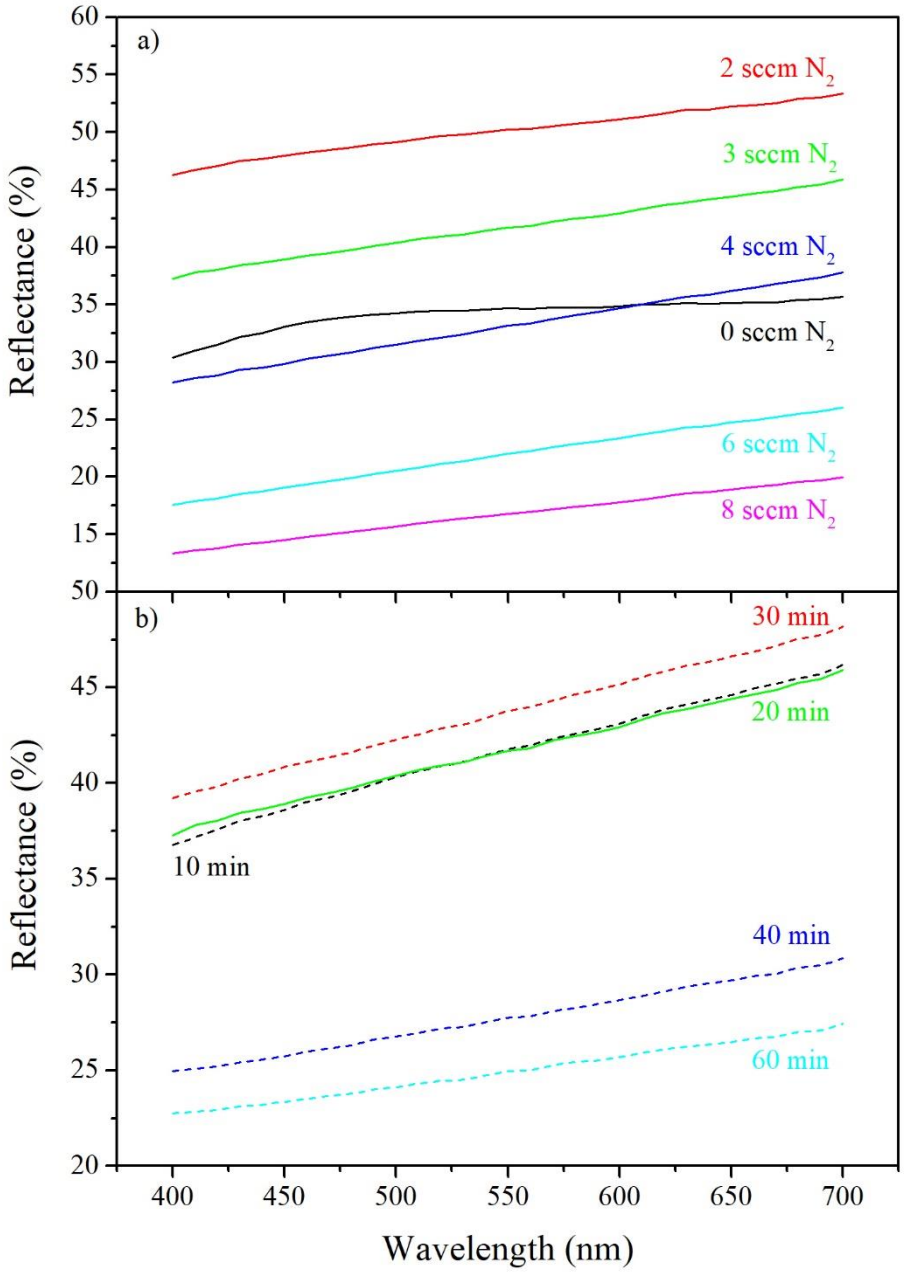

Figure 8

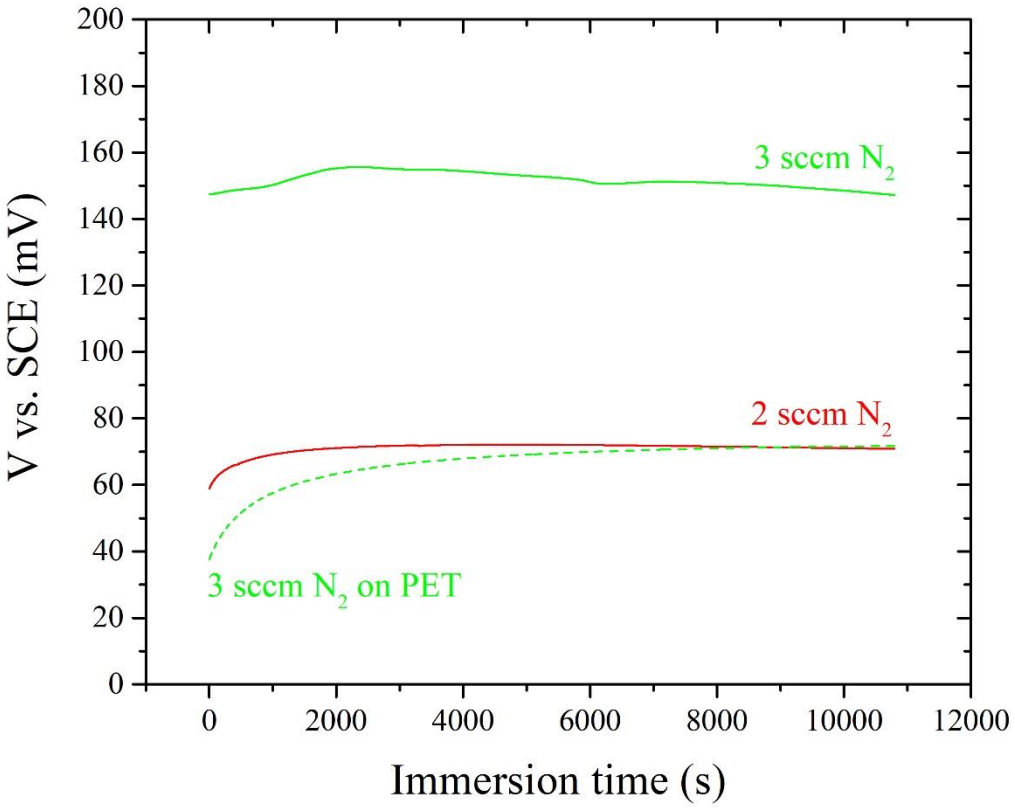

Figure 9

Plasma activation: 80 Pa Ar, 100 W, 300 s	
Deposition: 3 sccm N_2, 20 min	
PET before tape removal	**PET after tape removal**